Polymer Testing 53 (2016) 58–69

Contents lists available at ScienceDirect

Polymer Testing

journal homepage: www.elsevier.com/locate/polytest

Material properties

Evaluation of the rate of abiotic and biotic degradation of oxo-degradable polyethylene

Florencia Portillo [a], Oxana Yashchuk [b, c], Élida Hermida [a, b, c, *]

[a] Institute of Technology "Prof. Jorge A. Sabato", Av.Gral Paz 1499, B1650, San Martin, Argentina
[b] School of Science and Technology, National University of San Martin, Av. 25 de Mayo and Francia, B1650, San Martín, Argentina
[c] National Scientific and Technical Research Council, Av. Rivadavia 1917, 1033 Buenos Aires, Argentina

ARTICLE INFO

Article history:
Received 18 December 2015
Received in revised form
10 February 2016
Accepted 29 April 2016
Available online 12 May 2016

Keywords:
Polyethylene
Oxo-degradable
Photodegradation
Tensile test
Biodegradation

ABSTRACT

The recent introduction of oxo-degradable additive in the Argentinean market has motivated the study of the effect of abiotic (temperature and ultraviolet (UV) radiation) and biotic (aerobic in compost) degradation on the structure and mechanical behavior of films of polyethylene (PE) and oxo-degradable polyethylene (PE+AD).

Physico-chemical tests show that the failure strain and the carbonyl index of degraded PE and PE+AD samples depend on the UV irradiation dose. Furthermore, the additive plays a crucial role in the degradation and subsequent decay of the molecular weight.

It was observed that, for the same dose, the most deteriorated material was the one exposed to the lowest irradiance, emphasizing the importance of the time of exposure to UV radiation. The ratio between the irradiance and the critical dose, is a characteristic time associated to the sharp decay on the failure strain. The critical dose decreases significantly when increasing the temperature of the photodegradation assay.

PE is more susceptible to thermal degradation than PE+AD; the latter only degrades under thermal aging at the highest temperature.

Initially biotic degradation in compost showed an increasing production of carbon dioxide for both previously UV-degraded and untreated PE+AD. It is also remarkable that UV-degraded samples of PE and PE+AD with differences in their abiotic degradation level, reached the same final biotic degradation level. It was observed that although the additive increased the abiotic photodegradation, the molecular weight reduction in compost was not enough to reach the maximum biotic degradation level established by international standards for biodegradable materials.

1. Introduction

Plastics are very versatile materials that enable many applications due to properties such as flexibility, hardness, lightness; they are also excellent as a barrier against the permeation of gases, present various mechanical and physical properties, good optical properties (transparency) and ease of manufacture and molding of complex parts. Its increase in various applications (such as packaging, medical products and disposable items, auto parts, clothing, toys, etc.) has become a topic of vital importance in terms of its impact on the environment [1]. Firstly we must consider that these materials are produced from oil, natural gas and coal; despite being secondary products, their origin remains dependent on non-renewable sources such as fossil fuels. Second, the accumulation of waste of some inert plastics such as polyolefins, although not posing risk of ecotoxicity, generate major drawbacks [2].

It is worrying the longtime of plastic waste disposal, whose volume has increased dramatically in recent years (in the United States the generation of plastic solid waste increased 1500% in 30 years) [3]. 12.5% of the municipal solid waste (MSW) generated in the world are plastics (United Nations Program for the Environment UNEP, 2002), approximately 25 million tons per year; 50% of this amount comes from packaging [4]. In Argentina more than 12 million tons of municipal solid waste are generated annually (or an equivalent of 0.91 kg of waste per capita per day) of which 14± 4% are plastics. More than 25% of the waste generated is deposited in

* Corresponding author. School of Science and Technology, National University of San Martin, Av. 25 de Mayo and Francia, B1650HMQ, San Martín, Argentina.
E-mail address: oyashchuk@unsam.edu.ar (Hermida).

http://dx.doi.org/10.1016/j.polymertesting.2016.04.022
0142-9418/

open dumps and 30% in partial controlled landfills [5].

As already stated, the generation of solid waste is a conflict in every city in the world. In particular this work is based on the situation of plastic waste of the province of Buenos Aires, where more than 4 million tons/year of MSW (17%) are plastics [5]. To reduce their impact on the environment, in September 2008, the law 13868 of the Province of Buenos Aires (effective October 2009) was enacted. This legislation prohibits the use of plastic bags in supermarkets, warehouses and shops in general, and promotes such bags are replaced by those made of degradable materials so to reduce their environmental impact [6]. Under this legislation, traditional polyethylene bags were replaced by bags made from polyethylene and oxo-labeled as biodegradable, oxo-degradable or oxy-degradable. This attribute stems from the addition of special additives to standard thermoplastics in order to accelerate the degradation products. The first stage of degradation may be initiated by abiotic mechanisms including ultraviolet light (UV) of sunlight, heat or mechanical stress to promote the oxidation process. The hypothesis is that on breaking the molecular chain by oxidation the molecular weight becomes low enough to allow the action of microorganisms of the ecosystem where the plastic product was laid (biotic degradation or biodegradation).

Although the technology of oxo-degradable additives is not new, its appearance on the market raised questions about whether they are truly biodegradable according to international standards, such as EN13432 [7], EN14855 [8] and D5338 [9] for biodegradation in compost, for example. Recent contributions [10,11] remark disadvantages of oxo-degradable polymers: environmental fate of the polymer residues and possible accumulation of toxins, negative effect for polymer recycling—because the presence of oxo-degradable additives determines the life time of recycled products. Answers to these and other questions have to be established prior to accepting these polymers as environmentally friendly options.

Based on the problem of plastic waste management, this paper aims to determine whether the mechanical and structural properties are appropriate to characterize the kinetics of abiotic UV-degradation of polyethylene films with and without an oxo-degradable additive. Furthermore, another goal of the paper is to evaluate the susceptibility to biotic degradation, once these materials were subjected to abiotic degradation processes. In order to achieve these objectives, the effect of UV irradiation on the structure and mechanical behavior of polyethylene films with and without pro-degradant additives and its subsequent degradation in compost will be studied.

2. Materials and methods

2.1. Tested materials

For this work, polyethylene films (PE) and polyethylene films with the oxo-degradable additive $d_2w^{®}$ (PE+AD), both provided by RES Argentina, were considered. Films are white, and their thickness is about 50 μm.

Elemental analysis of samples was performed by X-ray fluorescence (XRF). A X-ray spectrometer wavelength dispersive flag 200 Panalytical Venus was used to evaluate the nature of the oxo-degradable additive by XRF. Fig. 1 shows the spectra of the blank, the PE and the PE+AD; the presence of titanium in both films is due to the addition of TiO_2 as a white pigment. Moreover the presence of manganese is observed only in the sample of PE + AD. Individual spectra for lighter elements in PE and PE+AD samples show a significant presence of Ca, and traces of K and Mg, as indicated in Table 1.

2.2. Photodegradation

Photodegradation was carried out in an environmental chamber Q-Lab Model QUV. This equipment simulates the harmful effects of solar radiation by UV fluorescent bulbs. It should be noted that although UV radiation accounts for only 5% of the sunlight that reaches the earth, it is responsible for the majority of solar degradation of polymeric materials exposed to the weather. Solar UV radiation can be divided into UVA, UVB and UVC, corresponding to long, medium and short wavelengths, respectively. This solar radiation reaching the earth 90% of UVA radiation, 10% of UVB, while 100% of the UVC radiation is filtered by the ozone layer. Therefore, in order to reproduce the long-wave UV radiation (UVA) for degradation testing. We use UVA-340 lamps, which offer the best correlation with the damage resulting from exposure outdoors, and simulating the solar spectrum between 295 nm and 365 nm with a maximum at 340 nm [12,13]. No condensation step was included.

PE and PE+AD films were cut into strips (250 ± 1) mm long (20 ± 1) mm wide and placed in sample holders into the environmental chamber for photodegradation at the temperatures and irradiances indicated in Table 2; these parameters were based on previous work [14–16] and can be set directly from the control panel of the chamber. Tests were carried out according to ASTM D-5208 [17]; samples were removed at different times in order to evaluate the physico-chemical changes due to the aging treatment.

2.3. Biotic degradation

Test samples of PE and PE+AD previously aged by UV radiation at 0.45 W/m^2 and 50 °C for 9 days (which the molecular weight was determined) and others aged at 0.89 W/m^2 and 70 °C for 96 hs (more degraded samples) were considered to assess the biotic degradation. Photodegraded samples (6.5 × 9.5) cm^2 were placed in compost stabilized bird guano in static 1000 ml glass containers at a constant temperature (55 ± 1) °C. Three samples were tested for each type of plastic films together with a positive control performed with quantitative filter paper (cellulose) and a blank; errors correspond to the standard deviation. In all containers cumulative production of CO_2 relative to the target was measured at regular intervals using the discontinuous method of determining CO_2 absorption in a potassium hydroxide solution and subsequent titration with hydrochloric acid.

2.4. Evaluation of the degradation effects

2.4.1. Cumulative carbon dioxide amount

The biodegradation percentage (D_t) of the test material for each measurement interval determined from the released cumulative amounts of CO_2 was calculated according to Eq. (1), where $(CO_2)_T$ was the cumulative amount of carbon dioxide evolved in each composting vessel; $(CO_2)_B$ was the mean cumulative amount of CO_2 evolved in the blank vessels; $ThCO_2$ was the theoretical amount of CO_2 produced by the test material.

$$D_t = \frac{(CO_2)_T - (CO_2)_B}{ThCO_2} \times 100 \quad (1)$$

2.4.2. Fourier transform infrared spectroscopy (FTIR)

The formation of carbonyl groups, typical feature of the polyethylene degradation, was evaluated by FTIR on a Nicolet Magna IR 560 equipment with a resolution of 2 cm^{-1} and 256 scans and dry air purge in the range of 600 cm^{-1} and 4500 cm^{-1}. Carbonyl index (CI) was determined as the ratio between the areas of the peaks at

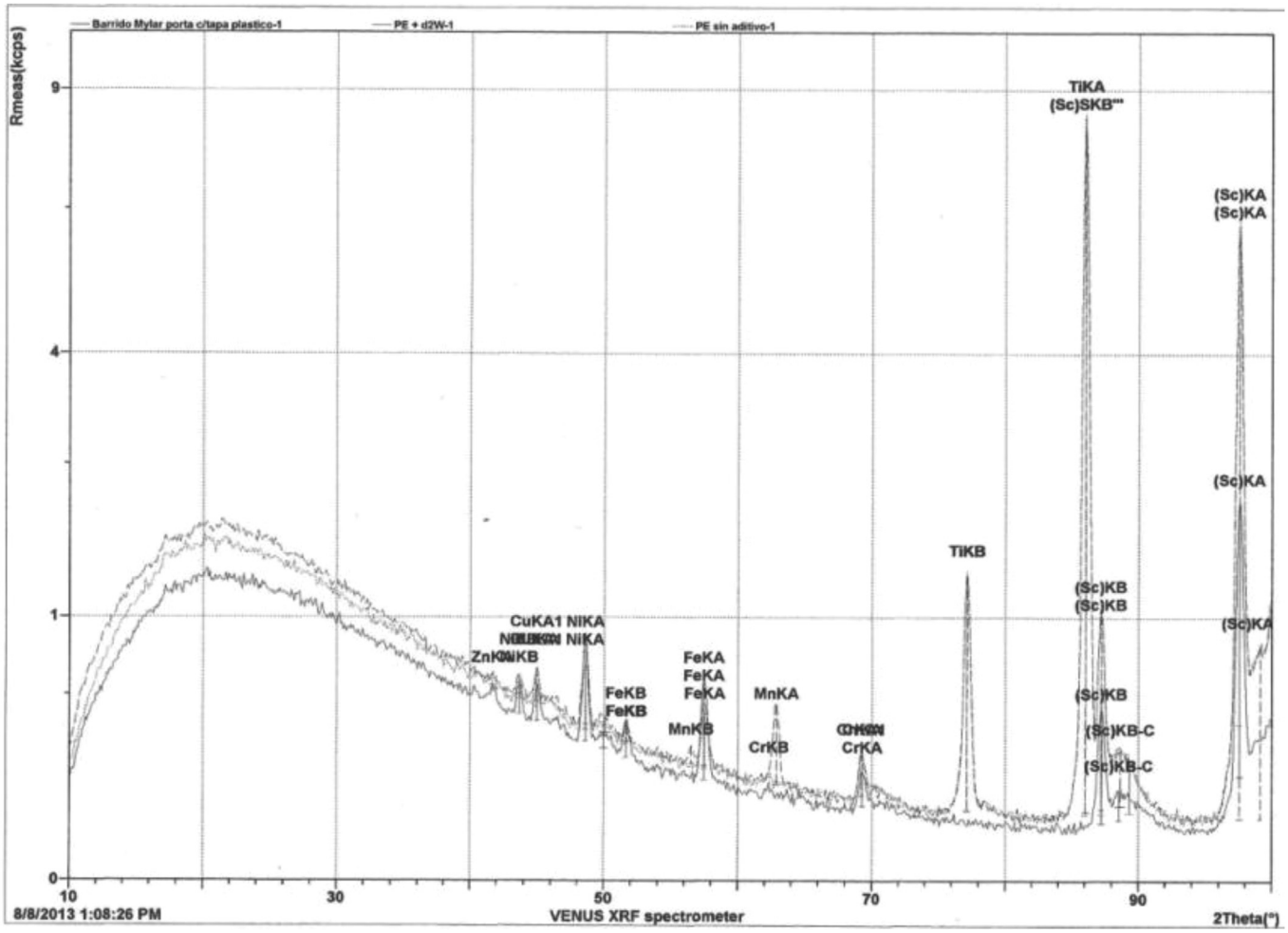

Fig. 1. FRX spectra for the blank (—), PE (···) and PE+AD (–).

Table 1
Intensity (arbitrary units) of the Ca, Mg and K peaks determined by XRF.

	PE	PE+AD
Ca	22.940	25.055
Mg	0.335	0.350
K	0.260	0.315

Table 2
Conditions for the accelerated UV degradation in the environmental chambers.

Test Nº	1	2	3	4	5
Irradiance [W/m^2]	0.35	0.45	0.89	0.89	1.20
Temperature [°C]	50	50	50	70	50

1715 cm^{-1} (corresponding to the formation of carbonyl groups during degradation) and the peak at 1460 cm^{-1} (corresponding to methylene groups).

In addition, a deconvolution of the carbonyl band (between 1650 cm^{-1} and 1800 cm^{-1}) was performed with the software Origin® 8.0 to determine the proportion of the various functional groups mentioned above.

2.4.3. Mechanical tests

Deterioration of the mechanical properties of PE and PE+AD photodegraded samples was evaluated using an Instron 1122 testing machine by tensile tests at a crosshead speed of 10 mm/min, according to ASTM D-3826 [18]. Specimens were cut parallel to the manufacturing direction of the film; they were (80 ± 1) mm long, (20 ± 1) mm wide and (50 ± 1) μm thick. Tensile modulus (initial slope of the tensile curve), stress at break and failure strain were determined at different periods of the degradation process.

2.4.4. Gel permeation chromatography (GPC)

As a result of the degradation processes polyethylene suffers a decrease in molecular weight, which was measured by a Waters Alliance 2000 GPC equipped with a refractive index detector and a viscometer and three columns: two 10 μm Plgel® Polymer Mixed B and one 10 μm with pore size of 10.6 nm.

Each sample was dissolved in 1,3,4-trichlorobenzene at 160 °C at a concentration 1.3 mg/ml. Tests were performed at 145 °C with a mobile phase of 150 μl of 1,3,4-trichlorobenzene at a flow rate of 1.0 ml/min. The system was previously calibrated using polystyrene.

2.4.5. Scanning electron microscopy (SEM)

FEI QUANTA microscopes Philips 200 and 515 were used to observe gold platted samples of pristine and photodegraded PE and PE+AD subjected to biotic degradation in compost.

3. Results

3.1. Mechanical behavior - embrittlement

Fig. 2 illustrates the tensile behavior of PE and PE+ AD samples subjected to an irradiance of 0.89 W/m^2 at 50 °C. Furthermore, Table 3 summarizes three main features of the mechanical response: the tensile modulus (E), the strain to failure (ε_b) and the ultimate stress (σ_b); they depend on the irradiance, temperature and extent of the abiotic degradation. For each condition of degradation, the mean value and the deviation were calculated using at least 5 tensile curves.

Fig. 3 shows that ε_b is the mechanical feature more sensitive to the degradation, for both PE and PE+AD, so ε_b is chosen to represent the mechanical degradation of the samples.

Fig. 4 shows how ε_b decreases as the dose increases: the initial value $\varepsilon_b^{initial}$ depends on the presence the additive, the decrease in ε_b is not monotonous but has an inflection point where the mechanical degradation is faster — the abscissa of this point is called D_C — and at large doses the elongation at break reaches a final value ε_b^{final}. The experimental data could be approximated by the sigmoidal shape given by Eq. (2) [19]:

$$\varepsilon_b = \varepsilon_b^{final} + \frac{\varepsilon_b^{initial} - \varepsilon_b^{final}}{1 + e^{\frac{Dose - D_C}{D_0}}} \quad (2)$$

The derivative of this equation has a maximum at the critical dose, D_C, that is, the abscissa of the inflection point. The value of the derivative at this maximum, i.e, the slope of the curve at the inflection point is given by Eq. (3).

$$\frac{\varepsilon_b^{initial} - \varepsilon_b^{final}}{4D_0} \quad (3)$$

Thus, D_0 (measured in kGy) is inversely proportional to the rate of the mechanical degradation.

According to Fig. 5 for any irradiance at a given radiation dose PE+AD degrades more than PE. Furthermore, this figure shows that for the same dose, both PE and PE+AD undergo more reduction of its mechanical properties (lower ε_b) at lower irradiance. That is, the time of exposure to UV radiation is a key factor for the mechanical degradation for both PE and PE+AD.

Finally Fig. 6 remarks the embrittlement (abrupt reduction of ε_b) of both PE and PE+AD samples as the temperature of the UV aging increases. Furthermore, a horizontal shift to lower doses is characteristic of a thermally activated process.

Table 4 summarizes the values D_C and D_0 obtained by fitting the experimental data according to Eq. (2).

3.2. FTIR – carbonyl index

A typical FTIR spectrum is shown in Fig. 7 (PE+AD irradiated with 0.45 W/m^2 at 50 °C). The main peaks correspond to the following functional groups: hydroperoxides (3200 cm^{-1}), alcohols (3416 cm^{-1}), ketones (1715 cm^{-1}), aldehyde (1725 cm^{-1}), carboxylic acids (1710 and 1715 cm^{-1}), noncyclic and cyclic esters (1735 cm^{-1}and 1785 cm^{-1}) and double bonds (909 cm^{-1}) [20]. For the same dose and temperature, the spectra of irradiated PE and PE+AD have no appreciable differences. In fact, for both materials the height of the absorption peaks of the degradation products increases as the time of exposure to UV radiation increases.

As pointed out in Section 2.4.2, the formation of carbonyl groups is the typical feature of the polyethylene degradation, thus the CI was determined for the irradiance, temperature and dose of each abiotic degradation by triplicate. The results are summarized in Table 5; CI, that is the proportion of carbonyl groups, increases as the exposure time increases.

Fig. 8 depicts CI versus dose; for a given treatment (temperature, irradiance and dose), the CI for PE+AD is greater than that for PE. Furthermore, both PE and PE+AD at the same dose, undergo further deterioration (CI increases) as the irradiance decreases. This feature, analogous to the mechanical behavior, remarks the deleterious effect of the time of irradiation.

In order to quantify the proportion of the different degradation products, the carbonyl band was fitted by 3 Lorentzian peaks according to the following Eq. (4):

$$y = \frac{2A_1}{\pi}\left(\frac{w_1}{4(x-1713)}\right)^2 + \frac{2A_2}{\pi}\left(\frac{w_2}{4(x-1741)}\right)^2 + \frac{2A_3}{\pi}\left(\frac{w_3}{4(x-1776)}\right)^2 \quad (4)$$

where A_i and w_i are the amplitude and width of peaks centered at: 1713 cm^{-1} for carboxylic acids and ketones, 1741 cm^{-1} for noncyclic esters and 1776 cm^{-1} for cyclic esters, peresters and lactones. Fig. 9 shows an example of the deconvolution and the proper fitting of the experimental spectra by the peaks given by Eq. (4), while Fig. 10 depicts the evolution of the area of each of the three deconvoluted peaks —normalized by the area of the peak at 1420 cm^{-1} — with the dose for PE and PE+AD irradiated at 0.35 W/m^2 to 50 °C. For both materials, the area of the peak associated to carboxylic acids and ketones (1713 cm^{-1}) increases with the dose more than the area of the peaks associated to esters, peresters and lactones do.

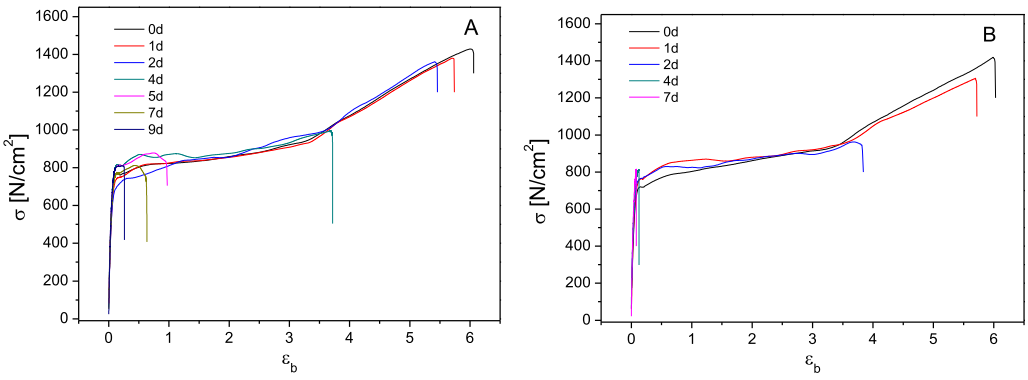

Fig. 2. Tensile curves, σ vs. ε, for PE (A) and PE+AD (B) films subjected UV irradiation at 0.89 W/m^2 and 50 °C during the indicated times.

Table 3
E, ε_b and σ_b for PE and PE+AD at the indicated irradiances and temperatures.

t [days]	Dose [kJ/m^2]	PE[a]	E [GPa]	ε_b	σ_b [MPa]	PE+AD[a]	E [GPa]	ε_b	σ_b [MPa]
0	0	1	0.100 ± 0.007	5.6 ± 0.2	13.7 ± 0.3	1	0.112 ± 0.005	5.9 ± 0.3	14.3 ± 0.8
3	91		0.147 ± 0.003	5.3 ± 0.4	16 ± 2		0.141 ± 0.005	4.63 ± 0.04	13.5 ± 0.4
6	181		0.162 ± 0.007	0.9 ± 0.2	9.6 ± 0.3		0.136 ± 0.008	4.5 ± 0.6	11 ± 1
9	272		0.159 ± 0.003	0.6 ± 0.1	9.7 ± 0.2		0.150 ± 0.004	0.7 ± 0.1	9.1 ± 0.2
12	363		0.206 ± 0.006	0.07 ± 0.03	10.1 ± 0.8		0.18 ± 0.02	0.12 ± 0.03	10.0 ± 0.7
15	454		0.225 ± 0.014	0.1 ± 0	10.9 ± 1		0.162 ± 0.007	0.2 ± 0.1	9.5 ± 0.4
0	0	2	0.100 ± 0.007	5.6 ± 0.2	13.7 ± 0.3	2	0.112 ± 0.005	5.9 ± 0.3	14.3 ± 0.8
1	39		0.122 ± 0.004	5.3 ± 0.2	14 ± 1		0.120 ± 0.006	4.7 ± 0.9	12 ± 2
2	78		0.127 ± 0.004	5.2 ± 0.6	14 ± 1		0.127 ± 0.003	4.9 ± 0.6	13 ± 2
4	156		0.123 ± 0.002	4.4 ± 0.7	12 ± 1		0.13 ± 0.02	0.57 ± 0.1	8.1 ± 0.9
6	233		0.126 ± 0.002	0.9 ± 0.2	8.5 ± 0.3		0.145 ± 0.007	0.24 ± 0.09	8.6 ± 0.2
9	350		0.138 ± 0.006	0.65 ± 0.03	8.8 ± 0.5		0.24 ± 0.01	0.03 ± 0.00	5.3 ± 0.1
0	0	3	0.100 ± 0.007	5.6 ± 0.2	13.7 ± 0.3	3	0.112 ± 0.005	5.9 ± 0.3	14.3 ± 0.8
1	77		0.119 ± 0.009	5.4 ± 0.6	14 ± 2		0.112 ± 0.006	5.6 ± 0.3	12.9 ± 0.4
2	154		0.11 ± 0.01	5.7 ± 0.4	14 ± 1		0.112 ± 0.009	4.1 ± 0.6	10 ± 1
4	308		0.128 ± 0.005	3.7 ± 0.9	11 ± 2		0.136 ± 0.007	0.1 ± 0.0	8.2 ± 0.4
5	384		0.139 ± 0.008	0.8 ± 0.3	8.7 ± 0.3		0.16 ± 0.01	0.08 ± 0.02	9.1 ± 0.8
7	538		0.128 ± 0.004	0.6 ± 0.1	8.0 ± 0.7		0.150 ± 0.004	0.08 ± 0.03	7.3 ± 0.9
	692		0.137 ± 0.007	0.23 ± 0.04	8.5 ± 0.4		–	–	–
0	0	5	0.100 ± 0.007	5.6 ± 0.2	13.7 ± 0.3	5	0.112 ± 0.005	5.9 ± 0.3	14.3 ± 0.8
1	104		0.147 ± 0.009	5.9 ± 0.4	17 ± 1		0.141 ± 0.005	4.63 ± 0.04	13.5 ± 0.4
2	207		0.142 ± 0.005	5.4 ± 0.7	16 ± 2		0.136 ± 0.008	4.5 ± 0.6	11 ± 1
3	311		0.149 ± 0.009	4.8 ± 0.8	14 ± 1		0.150 ± 0.004	0.7 ± 0.1	9.1 ± 0.2
4	415		0.148 ± 0.004	4.6 ± 0.4	13 ± 1		0.18 ± 0.02	0.12 ± 0.03	10.0 ± 0.7
5	518		0.146 ± 0.007	0.6 ± 0.2	8.8 ± 0.6		0.162 ± 0.007	0.2 ± 0.1	9.5 ± 0.4
0	0	4	0.100 ± 0.007	5.6 ± 0.02	13.7 ± 0.3	4	0.112 ± 0.005	5.9 ± 0.3	14.3 ± 0.8
0.3	26		–	–	–		0.154 ± 0.009	2.9 ± 0.6	9.3 ± 0.7
0.7	51		–	–	–		0.17 ± 0.02	0.3 ± 0.2	10 ± 1
1	77		0.143 ± 0.006	4.3 ± 0.8	12 ± 2		0.169 ± 0.008	0.13 ± 0.03	9.6 ± 0.1
2	154		0.155 ± 0.007	0.9 ± 0.2	8.9 ± 0.3		0.26 ± 0.04	0.0 ± 0	6 ± 2
3	231		0.149 ± 0.006	0.33 ± 0.05	8.6 ± 0.3		0.181 ± 0.009	0.03 ± 0.01	5.7 ± 0.6
4	308		0.163 ± 0.008	0.19 ± 0.06	9.2 ± 0.3		0.14 ± 0.01	0.03 ± 0.00	4.1 ± 0.2
5	384		0.156 ± 0.008	0.1 ± 0	9.5 ± 0.6		–	–	–

[a] Numbers correspond to for the accelerated UV degradation treatment shown in Table 2.

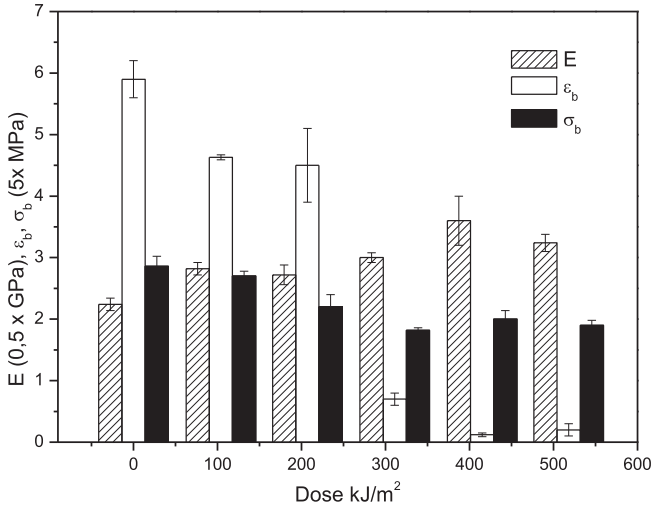

Fig. 3. E, ε_b and σ_b of PE+AD films degraded by UV radiation at 1.20 W/m^2 and 50 °C vs. dose.

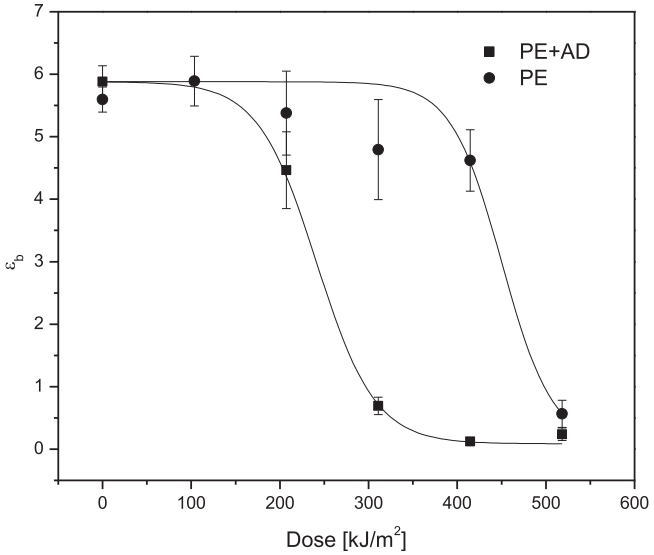

Fig. 4. ε_b vs dose for PE (●) and PE+AD (■) subjected to UV radiation at 1.20 W/m^2 and 50 °C.

3.3. GPC — molecular weight decrease

PE and PE+AD degraded at an irradiance of 0.45 W/m^2 at 50 °C presented the more gradual change in the CI for doses up to 350 kJ/m^2, as depicted in Fig. 8. Therefore, samples irradiated at 0.45 W/m^2 at 50 °C were chosen to follow the evolution of the molecular weight with the irradiation dose; this evolution is presented in Fig. 11.

Regarding PE, as the time of irradiation increases the distribution shifts slightly towards lower molecular weight, keeping its bell-shape. However, for PE+AD not only the shift of the distribution to lower molecular weights is more pronounced, but also a

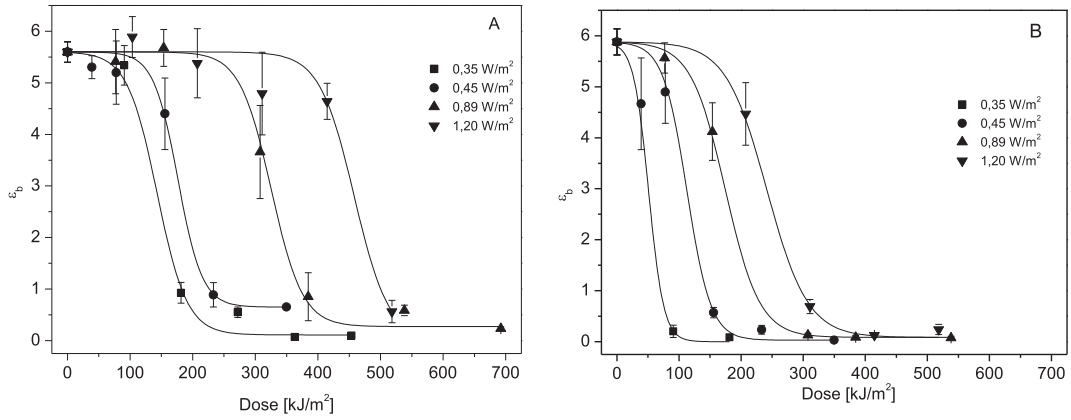

Fig. 5. ε_b vs dose at different irradiances at 50 °C for PE (A) and PE+AD (B).

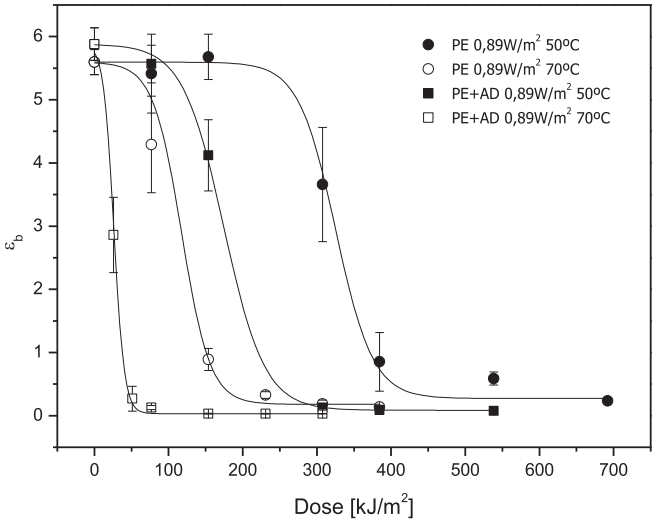

Fig. 6. ε_b vs dose for PE and PE+AD subjected to an UV irradiance of 0.89 W/m^2 at 50 and 70 °C.

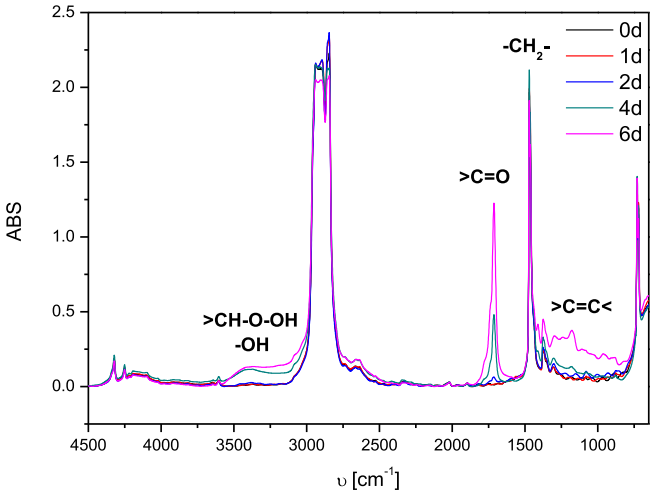

Fig. 7. FTIR spectrum for irradiated PE+AD at 0.45 W/m^2 and 50 °C.

Table 4
Parameters D_C and D_0 used to fit the experimental data ε_b vs dose by Ec. (2).

T [ºC]	Irradiance [W/m^2]	PE		PE+AD	
		D_C [kJ/m^2]	D_0 [kJ/m^2]	D_C [kJ/m^2]	D_0 [kJ/m^2]
50	0.35	143 ± 22	24 ± 12	51 ± 5	12 ± 1
	0.45	175 ± 8	22 ± 2	112 ± 18	19 ± 2
	0.89	325 ± 23	25 ± 8	175 ± 3	28 ± 1
	1.20	457 ± 6	27 ± 3	241 ± 11	33 ± 5
70	0.89	118 ± 8	19 ± 6	26 ± 4	7 ± 2

narrowing of the distribution with increasing the time of exposure to the UV radiation is observed. Furthermore, a shoulder at molecular weights of about 500 Da appears after 48 hs of irradiation and increases at greater doses.

Fig. 12 represents the number average molecular weight, M_n, against the dose. There is a decrease in the molecular weight of PE with an inflection point around 100 kJ/m^2 and an asymptotic limit at 12 kDa; for PE+AD there is a faster decrease in M_n with an inflection point around 75 kJ/m^2 and an asymptote about 2 kDa. These experimental data can be fitted by Eq. (5):

$$M_n = M_n^{final} + \frac{M_n^{initial} - M_n^{final}}{1 + e^{\frac{Dose - D_C}{D_0}}} \quad (5)$$

This equation has the same functional dependence as the one used to fit the experimental data of ε_b vs. dose. Table 6 present the values obtained for the setting of this parameter according to Eq. (5).

3.4. Biodegradation

In the first experiment the samples were pre-exposed to UV radiation of 0.89 W/m^2 at 70 °C for 96 h. This abiotic degradation with an irradiation dose of 308 kJ/m^2 produced the higher decline of the mechanical properties and the greater increase of the CI among the aging treatments presented in this work. At the beginning of the experiment a similar CO_2 accumulation in the glass containers with cellulose and PE samples was observed, while the biodegradation rate was faster in the containers with PE + AD samples (Fig. 13A). This high microbial activity associated with PE+AD samples might be attributed to the presence of the low molecular weight chains as well as to the additive and the high value of CI obtained after abiotic treatment.

Table 5
Carbonyl index of PE and PE+AD subjected to UV irradiation at the indicated irradiance, temperature and dose.

t [days]	Dose [kJ/m^2]	PE[a]	CI	PE+AD[a]	CI
0	0	1	0	1	0
3	91		0.031 ± 0.005		0.016 ± 0.002
6	181		0.11 ± 0.02		0.63 ± 0.09
9	272		0.16 ± 0.02		0.9 ± 0.1
12	363		0.16 ± 0.02		1.3 ± 0.2
15	454		0.24 ± 0.04		2.4 ± 0.4
0	0	2	0	2	0
1	39		0.0059 ± 0.0009		0.0004 ± 0.0001
2	78		0.012 ± 0.002		0.045 ± 0.007
4	156		0.041 ± 0.006		0.41 ± 0.06
6	233		0.06 ± 0.009		0.8 ± 0.1
9	350		0.17 ± 0.03		1.4 ± 0.2
0	0	3	0	3	0
1	77		0.0036 ± 0.0005		0.039 ± 0.006
2	154		0.04 ± 0.006		0.29 ± 0.04
4	308		0.10 ± 0.01		0.57 ± 0.09
5	384		0.13 ± 0.02		0.9 ± 0.1
7	538		0.22 ± 0.03		1.4 ± 0.2
9	692		0.27 ± 0.04		1.9 ± 0.3
0	0	5	0	5	0
1	104		0.008 ± 0.001		0.0021 ± 0.0003
2	207		0.009 ± 0.001		0.013 ± 0.002
3	311		0.049 ± 0.007		0.56 ± 0.08
4	415		0.09 ± 0.01		0.9 ± 0.1
5	518		0.20 ± 0.03		0.6 ± 0.09
0	0	4	0	4	0
0.3	26		–		–
0.7	51		–		0.17 ± 0.03
1	77		0.09 ± 0.01		1.0 ± 0.1
2	154		0.18 ± 0.03		1.8 ± 0.3
3	231		0.24 ± 0.04		2.6 ± 0.4
4	308		0.59 ± 0.09		5.6 ± 0.8
5	384		1.4 ± 0.2		6.3 ± 0.9

[a] Numbers correspond to for the accelerated UV degradation treatment shown in Table 2.

After 15 days of incubation, however, the biodegradation in the containers with PE + AD samples reached a plateau that lasted 10 days, and then the biodegradation matched the curve of PE samples biodegradation. After 60 days of incubation the CO_2 accumulation reached plateau again, where the CO_2 production in the containers with samples was equal to that of the blank experiment. About 23% of biodegradation took place for both types of samples during 90 days of experiment.

In the second experiment samples were pre-exposed to UV radiation of 0.45 W/m^2 at 50 °C for 216 h (the total irradiance dose = 350 kJ/m^2) and then their molecular weight was determined. The M_n and M_w values were 1.6 kDa and 6.0 kDa for PE+AD samples and 11.6 kDa and 106.2 kDa for PE samples, respectively. Moreover, the biotic degradation of untreated PE + AD samples (M_n = 17.3 kDa and M_w = 239 kDa) was studied to establish the effect of previous abiotic treatment on the biotic degradation.

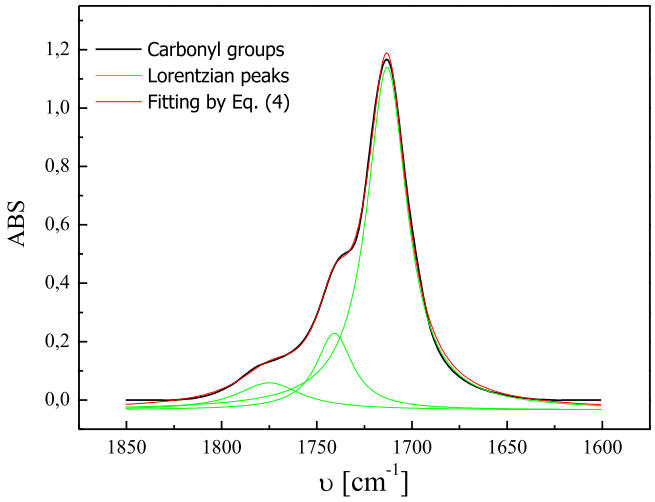

Fig. 9. FTIR in the region of carbonyl groups for PE+AD under irradiance of 0.45 W/m^2 and 50 °C after 9 days.

The CO_2 accumulation along 120 days of incubation is illustrated in Fig. 13B. Since the dose was very close to the one applied in the first experiment, the final biodegradation degree for the PE+AD irradiated sample was very similar for both tests. As in the previous experiment, at the beginning of the test CO_2 accumulation rate was faster in the containers with previously abiotic degraded PE+AD than with untreated PE+AD. Furthermore, these latter samples showed higher biodegradation rate than abiotic degraded PE samples.

However, between 30 and 60 days, the degree of biodegradation of the untreated PE + AD samples was higher than for the irradiated PE+AD samples. Finally, the process reached a plateau (at a dose D_t) after 60, 100 and 110 days for untreated PE + AD (D_t = 6%), previously abiotic degraded PE (D_t = 4%) and PE + AD samples (D_t = 21%), respectively.

3.5. SEM - morphology

Fig. 14 shows micrographs of the surface of PE and PE+AD

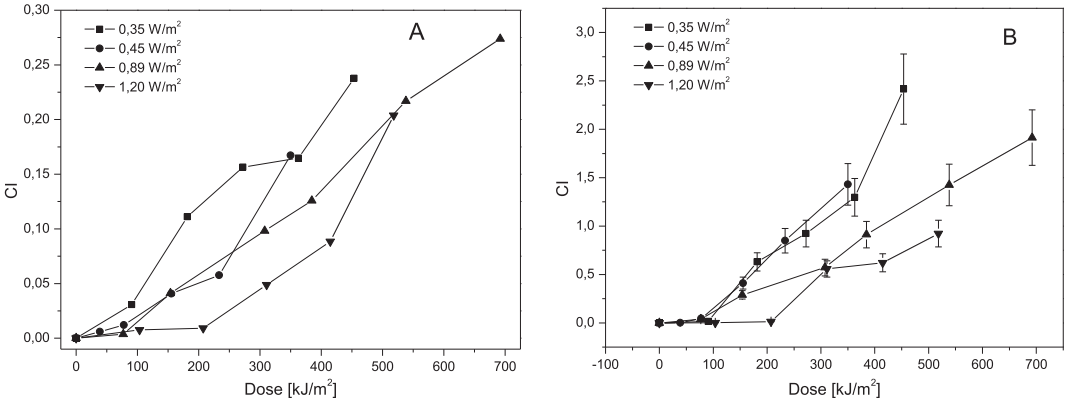

Fig. 8. CI vs dose at different irradiances at 50 °C for PE (A) and PE+AD (B). Note the change of scale in the CI.

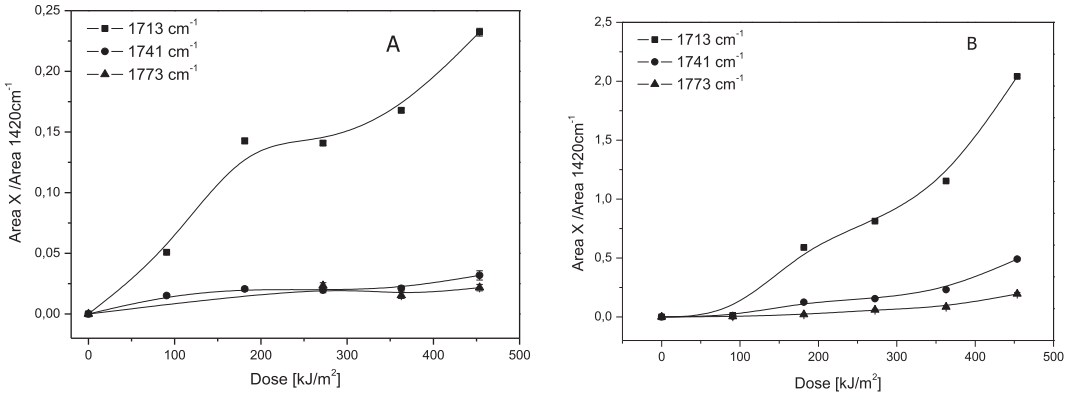

Fig. 10. Height of the Lorentzian peaks centered at the wavenumber indicated by the labels, for PE (A) and PE+AD (B) irradiated at 0.35 W/m^2 and 50 °C. Note that the vertical scales are different.

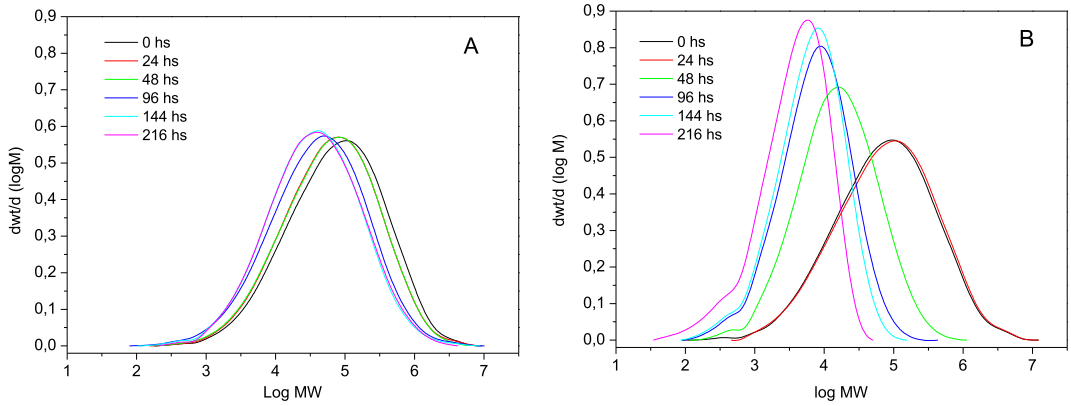

Fig. 11. Changes in the molecular weight distribution of PE (A) and PE+AD (B) subjected to UV radiation at 0.45 W/m^2 and 50 °C at the indicated irradiation times. For PE some distributions overlaps.

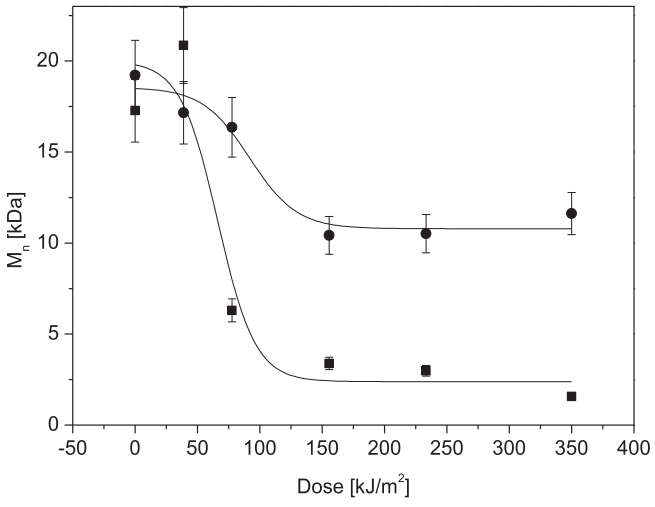

Fig. 12. M_n vs. dose for PE (●) and PE+AD (■) samples irradiated at 0.45 W/m^2 and 50 °C. M_n data are fitted using Eq. (5).

samples before and after abiotic degradation at 0.45 W/m^2, 50 °C during 9 days (total dose: 350 kJ/m^2). No differences were observed between the untreated PE and the abiotic degraded PE surfaces while the PE+AD surface was slightly chopped after photodegradation. Furthermore, the surface of PE+AD submitted to degradation in compost during 90 days, exhibited extensive surface erosion and adhered bacterial colonies on the surface; by comparison PE samples showed no surface damage after composting and virtually no colonies (Fig. 14c).

Table 6
Parameters D_C and D_0 used to fit M_n vs. dose curves by Eq. (5).

Irradiation condition	PE		PE+AD	
	D_C [kJ/m^2]	D_0 [kJ/m^2]	D_C [kJ/m^2]	D_0 [kJ/m^2]
0.45 W/m^2, 50 °C	92 ± 9	18 ± 2	67 ± 9	15 ± 2

4. Discussion

The evolution of the mechanical response (Fig. 5) and the CI (Fig. 8) with the UV-irradiation dose for both PE and PE+AD has shown that the degradation increases as the irradiance decreases. This means that the time of exposure to radiation is the key parameter for the photodegradation. Furthermore Fig. 15 shows that, within the experimental error, the critical dose at which a significant decay of the mechanical properties is observed, D_C is proportional to the irradiance. Such proportionality is given by a characteristic time (the slope of the line) that is lower for the PE + AD than for PE. This implies that the additive acts by promoting the degradation and consequently decreasing the time at which the mechanical properties decay abruptly. D_0 that is inversely proportional to the slope with which the break strain

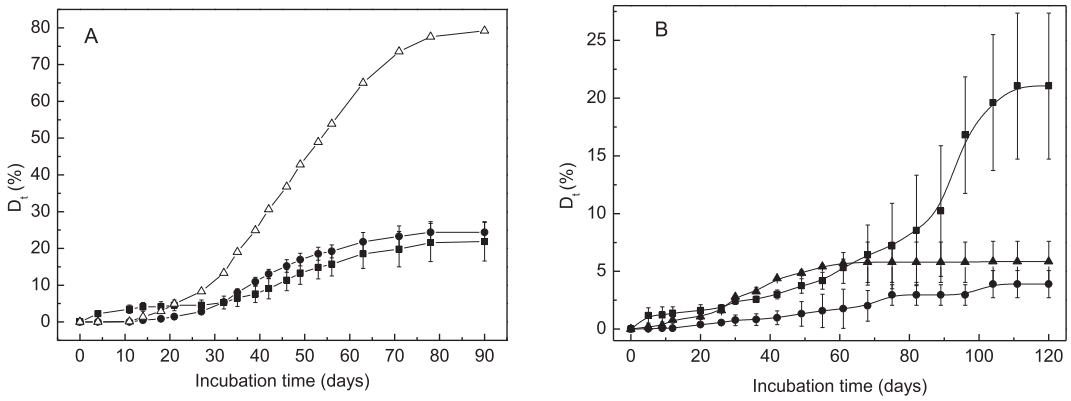

Fig. 13. Aerobic biodegradation degree of untreated PE+AD (▲), cellulose (Δ) and PE (●), PE+AD (■) films pre-exposed to ultraviolet and thermal treatment at: A) 0.89 W/m^2 and 70 °C for 4 days; B) 0.45 W/m^2 and 50 °C for 9 days.

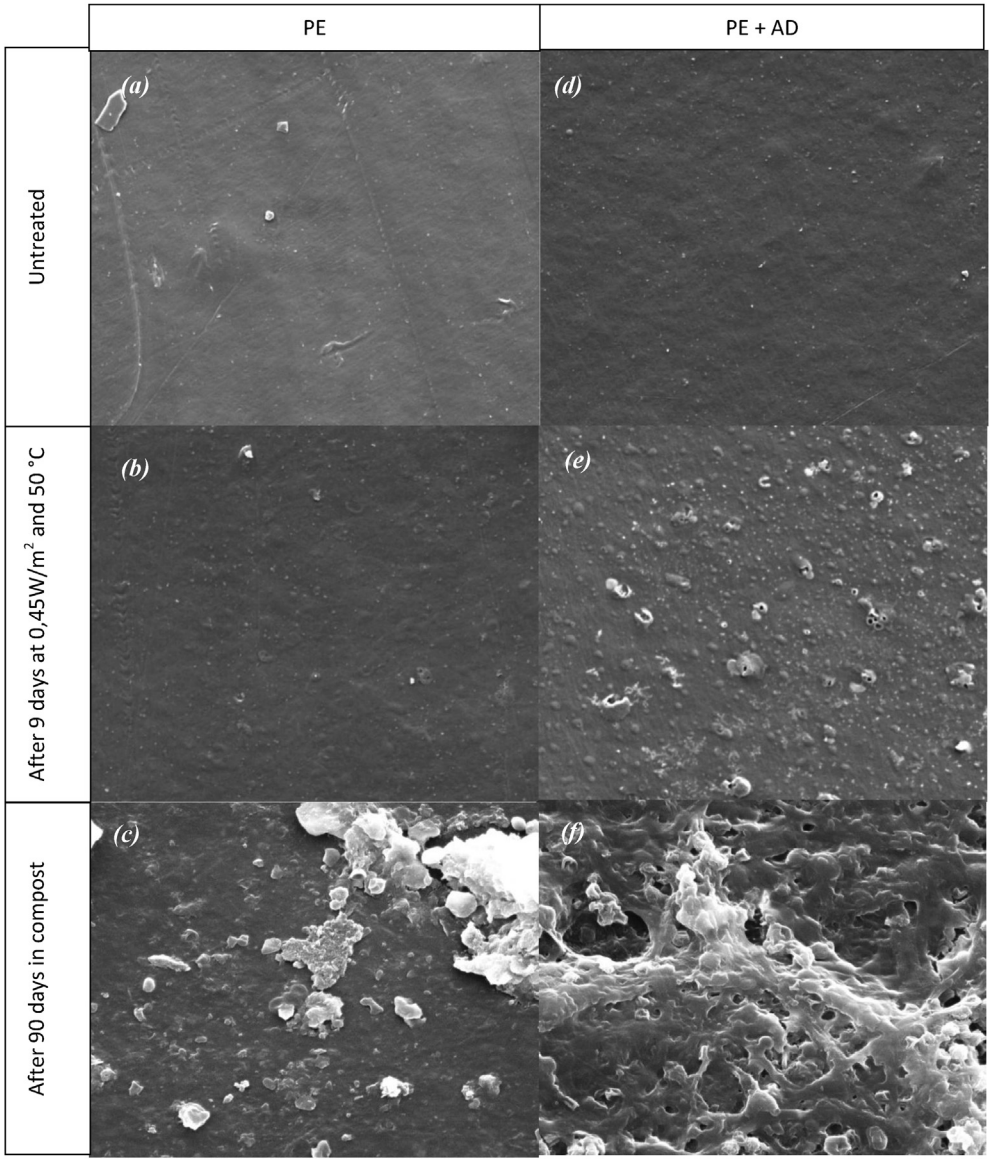

Fig. 14. Surface of PE and PE+AD samples, untreated (a,d), irradiated 9 days at 0.45 W/m^2 and 50 °C (b,e) and after 90 days in compost post irradiation (c,f) (× 4000).

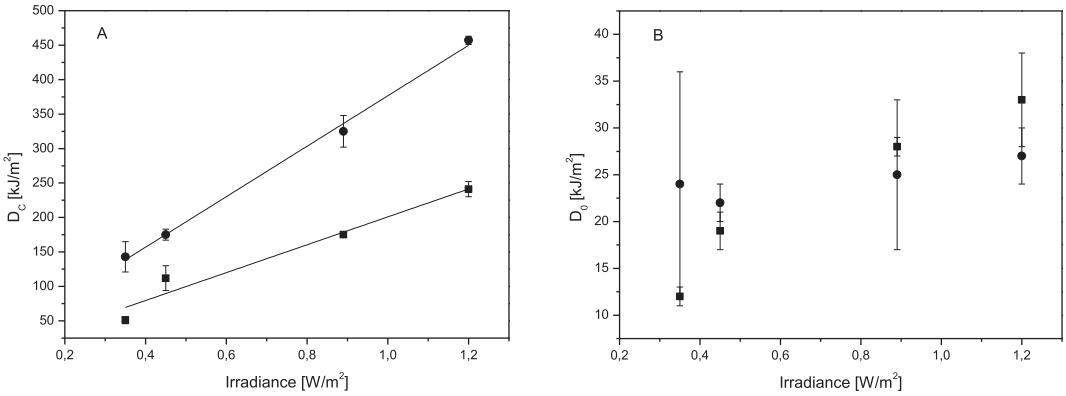

Fig. 15. D_C (A) and D_0 (B) vs. irradiance for PE (●) and PE+AD (■) samples.

decays as a function of the dose, is almost a constant parameter for PE, while for PE + AD the higher the irradiance the slower its decay, as depicted in Fig. 15.

Regarding changes in the molecular weight illustrated in Fig. 12, at the beginning of the exposure to UV radiation, the additive produced a greater decrease in the molecular weight of PE+AD than of PE. However, after exceeding 75 kJ/m^2 (2 days of exposure at 0.45 W/m^2) the same slope in the decrease of M_n was achieved for both PE and PE + AD. Therefore, at this stage the degradation of both materials might be due to the same mechanism, regardless the presence of the additive.

One goal of this work has been to correlate changes in the mechanical response, assessed by ε_b, with structural changes in the irradiated material, measured by the IC and M_n. The analysis of ε_b vs. dose showed that the additive lowers the time required to reach the critical dose, that is, the additive significantly accelerates the oxidation of the material.

The decrease in molecular weight shows that the action of the additive occurs in the early stages of the degradation, producing a rapid initial decay of the molecular weight, but after a certain time of irradiation the additive loses its effect. This behavior can be explained considering that the additive contains mainly manganese (Fig. 1); this transition metal acts by promoting the decomposition of hydroperoxides. These hydroperoxides, initially formed by thermal oxidation and mechanical stresses while blowing the films, exhausted and therefore limited the photodegradation rate. Afterwards, the degradation of PE+AD advances through the action of free radicals already present in the PE or being produced by the UV degradation, i.e. the same degradation mechanisms as for PE (without additive).

The depletion of hydroperoxides produced a slow down in the degradation with a consequent decrease in the slope of the decay of the mechanical properties vs dose. Fig. 16 compares the values for D_C and D_0 used to fit ε_b vs dose (Table 4) and M_n vs dose (Table 6) both at 0.45 W/m^2 at 50 °C. D_0 is not much sensitive neither to the additive nor to the property under consideration (molecular weight or failure strain). However, for both PE and PE+AD, the critical dose D_C is much lower for the M_n data than for the mechanical response; that is, the molecular weight decreases earlier than the failure strain due to the photodegradation, as illustrated in Fig. 17.

The CI has a strong dependence on the molecular weight only below 6 kDa, as shown in Fig. 18. Thus, CI is not a proper indicator of the early stages of degradation but suitable for monitoring the degradation parameter in advanced stages.

Regarding the biodegradation kinetics depicted in Fig. 13, PE+AD samples with similar UV-dose (300–350 kJ/m^2) but different abiotic degradation temperatures reached plateaux with very similar ultimate values (approximately 22%) but at different times: 60 days (Fig. 13A) or 110 days (Fig. 13B). This feature points out that biodegradation is controlled by a thermally activated process.

The high initial level of the biotic degradation of pretreated and

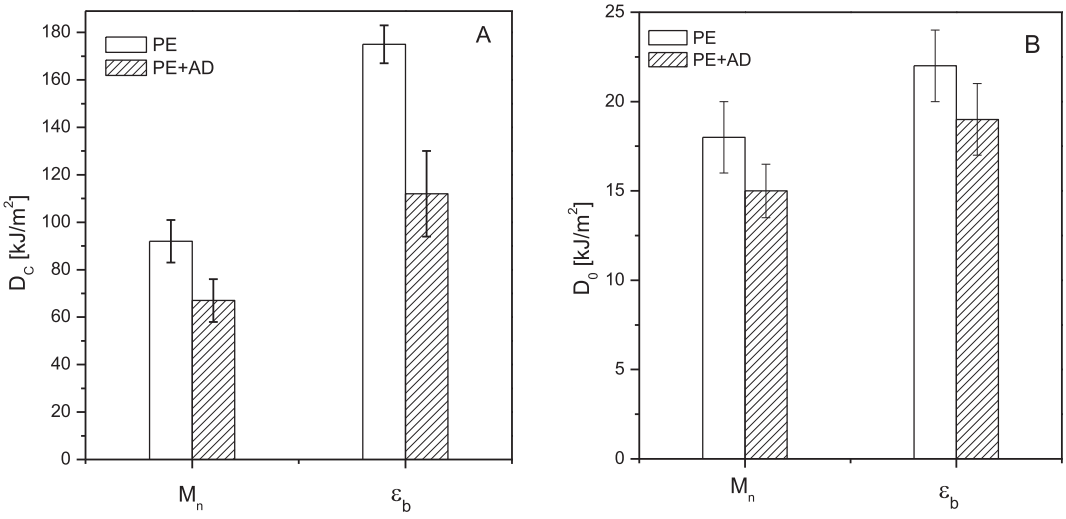

Fig. 16. D_C (A) y D_0 (B) used to fit ε_b vs. dose and M_n vs. dose data for PE y PE+AD samples irradiated at 0.45 W/m^2 and 50 °C.

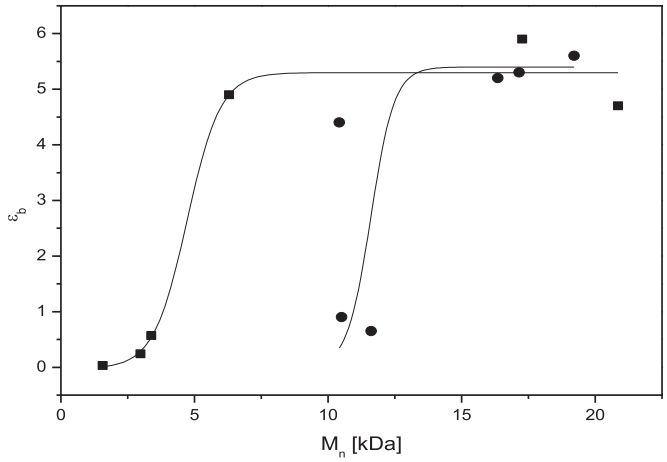

Fig. 17. M_n vs. ε_b for PE (●) and PE+AD (■) samples irradiated at 0.45 W/m^2 and 50 °C.

untreated PE + AD samples with respect to PE samples might be due to the additive, which acts as nutrient for the microorganisms. Husarova et al. [21] observed that the presence of $CaCO_3$ as an additive greatly increased the CO_2 accumulation in glass containers, but did not enhance the abiotic degradation of the films. This could also occur in our experiments, since calcium was detected in the PE+AD samples according to Section 2.1. Therefore, during the biodegradation in compost, the reaction $CO_3^{2-} + 2H^+ \rightarrow CO_2 + H_2O$ might be responsible of the initial CO_2 accumulation.

Finally, the presence of colonies of microorganisms and biofilm formation on the surface of PE+AD samples was detected. However this is not an indication of the biodegradation process. Although the material degrades in compost, the ultimate value reached after 90 days in compost (around 22%) is too low compared to the values stated in international standards of biodegradation in compost (90%) [8]. Therefore, the oxo-degradable additive cannot assure the biodegradation of PE.

5. Conclusions

The presence of the oxo-degradant additive promotes the degradation of the polyethylene samples by effect of the UV irradiation. This degradation produces structural changes such as the decrease in molecular weight of the polymer, specially at the early stages of the biotic degradation, and the generation of oxidation products detectable by monitoring the rate of carbonyls at high degradation times.

The dependence of the strain to failure and the molecular weight with the irradiation dose could be fitted by sigmoidal empirical fittings, characterized by a critical dose D_C and a degradation factor D_0.

It was established that D_C is proportional to the irradiance; the proportionality constant can be regarded as a characteristic time. This time, lower for PE+AD than for PE, remarks the photodegradation effect of the oxo-degradable additive.

The additive acts at the early stages of degradation, producing a rapid decay of molecular weight at the beginning. This behavior was attributed to the presence of manganese that promotes the decomposition of hydroperoxides until its depletion.

Finally, although the additive substantially promotes the photodegradation of PE, this degradation is not enough, neither in the more severe condition of irradiation (CI 0.59 for PE and 5.6, for PE+AD), to produce a decrease in the molecular weight that enables composting. In fact, both materials reached the same level of biotic degradation. Therefore photodegraded PE+AD cannot be considered biodegradable and does not constitute a solution to the accumulation of municipal solid waste.

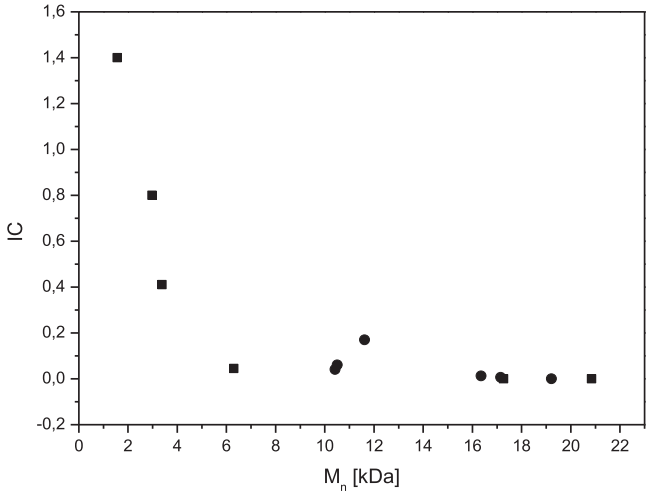

Fig. 18. M_n vs. CI for samples irradiated at 0.45 W/m^2 and 50 °C.

Acknowledgements

We thank RES Argentina for having provided the PE and PE+AD films used in this work and Dr. Rafael García and Dr. Carlos Domínguez (Laboratory of Polymer Technology, Universidad Rey Juan Carlos, Spain) for the determination of the molecular weight distributions by GPC.

This research has been partially supported by the National Agency for the Promotion of Science and Technology, Argentina. O. Yashchuk and F. Portillo thanked CONICET and CNEA, respectively, for their research fellowships.

References

[1] B. Singh, N. Sharma, Mechanistic implications of plastic degradation, Polym. Degrad. Stab. 93 (2008) 561–584.
[2] M. Koutny, J. Lemaire, A.M Delort, Biodegradation of polyethylene films with prooxidant additives, Chemosphere 64 (2006) 1243–1252.
[3] E.S. Stevens, Green plastics: an Introduction to the New Science of Biodegradable Plastics, Princeton University Press, USA, 2002.
[4] United States Enviromental Protection Agency. http://www3.epa.gov/ (accessed November 2015).
[5] National project for the integrated management of municipal solid waste in Argentina. http://www.ambiente.gov.ar/archivos/web/PGC/File/EAS%20(1,91MB).pdf (accessed November 2015).
[6] The Buenos Aires Province Legislature. http://www.gob.gba.gov.ar/intranet/digesto/PDF/l13868.pdf (accessed November 2015).
[7] UNE-EN 13432, Requirements for Packaging Recoverable through Composting and Biodegradtion. Test Scheme and Evaluation Criteria for the Final Acceptance of Packaging, 2001.
[8] UNE-EN ISO 14855, Determination of the Ultimate Aerobic Biodegradability of Plastic Materials under Controlled Composting Conditions. Method by Analysis of Evolved Carbon Dioxide, 2013.
[9] ASTM D5338-15 Standard Test Method for Determining Aerobic Biodegradation of Plastic Materials under Controlled Composting Conditions, Incorporating Thermophilic Temperatures.
[10] S. Fontanella, S. Bonhomme, J.-M. Brusson, S. Pitteri, G. Samuel, G. Pichon, J. Lacoste, D. Fromageot, J. Lemaire, A.-M. Delort, Comparison of biodegradability of various polypropylene films containing pro-oxidant additives based on Mn, Mn/Fe or Co, Polym. Degrad. Stab. 98 (2013) 875–884.
[11] P.K. Roy, M. Hakkarainen, I.K. Varma, A.-C. Albertsson, Degradable polyethylene: fantasy or reality, Envir Sci. Technol. 45 (2011) 4217–4227.
[12] Q-Lab LU-0822, Technical Bulletin- Sunlight, Weathering and Light Stability, 2011. http://www.q-lab.com/documents/public/cd131122-c252-4142-86ce-5ba366a12759.pdf (accessed November 2015).
[13] Q-Lab LU-8032, Technical Bulletin-Irradiance Control in Fluorescent UV Exposure Testers, 2011. http://www.q-lab.com/documents/public/e0f2b395-6d93-41d3-804a-f18e233c8f2d.pdf (accessed November 2015).

[14] J.V. Gulminea, P.R Janissekb, H.M. Heisec, L. Akcelrud, Degradation profile of polyethylene after artificial accelerated weathering, Polym. Degrad. Stab. 79 (2003) 385–397.
[15] ASTM D4587-11 Standard practice for fluorescent UV-condensation exposures of paint and related coatings.
[16] A. Krzan, S. Hemjinda, S. Miertus, A. Corti, E. Chiellini, Standardization and certification in the area of environmentally degradable plastics, Polym. Degrad. Stab. 91 (2006) 2819–2833.
[17] ASTM D5208-09 Standard Practice for Fluorescent Ultraviolet (UV) Exposure of Photodegradable Plastics.
[18] ASTM D 3826–98, Standard Practice for Determining Degradation End Point in Degradable Polyethylene and Polypropylene Using a Tensile Test, 2008.
[19] E.B. Hermida, V.I. Mega, O. Yashchuk, V. Fernández, P. Eisenberg, S.S Miyazaki, Gamma irradiation effects on mechanical and thermal properties and biodegradation of poly(3-hydroxybutyrate) based film, Macromol. Symp. 263 (2008) 102–113.
[20] J.V. Gulmine, P.R Janissek, H.M. Heise, L. Akcelrud, Polyethylene characterization by FTIR, Polym. Test. 21 (2002) 557–563.
[21] L. Husarova, M. Machovsky, P. Gerych, J. Houser, M. Koutny, Aerobic biodegradation of calcium carbonate filled polyethylene films containing pro-oxidant additives, Polym. Degrad. Stab. 95 (2010) 1794–1799.